Staff Summary Sheet

	To	Action	Signature (Surname), Grade, Date		To	Action	Signature (Surname), Grade, Date
1	DFER	Review	SoLTS, AD25, 28Sept15	6			
2	Dr York	Action		7			
3				8			
4				9			
5				10			

Grade and Surname of Action Officer	Symbol	Phone	Suspense Date
Dr York	DFEC	333-4210	9 Oct 2015

Subject		SSS Date
Clearance of Material for Public Release	Case Number: USAFA-DF-PA-353	24 Sep 2015

Summary

1. Purpose: To provide security and policy review on the paper at Tab 1 prior to release to the public.

2. Background:

- *Author(s)*: Chimpalthradi R. Ashokkumar and George W.P. York. (DFEC, x4210)
- *Title*: "LQR for in situ discrete structural damage growth retardation"

- *Release information*: Journal article to be published in the *IEEE Transactions on Control Systems Technology*

- *Previous clearance information*: None.

- *Recommended distribution statement*: Distribution A, Approved for public release, distribution unlimited.

3. Recommendation: Sign coord block above indicating document is suitable for public release. Suitability is based solely on the document being unclassified, not jeopardizing DoD interests, and accurately portraying official policy.

George York

Dr George York
UAS Research Center
Department of Electrical and Computer Engineering

Tab
1. Copy of Paper

LQR for in situ discrete structural damage growth retardation

Chimpalthradi R. Ashokkumar[1] and George WP York[2]
US Air Force Academy, 2354 Fairchild Dr, Ste 2F6, Colorado Springs, CO 80840-6236.

ABSTRACT

One of the objectives in structural health monitoring is damage localization and assessment. During service intervals, damages are localized; however, assessment (the sizes of damages) is generally difficult to determine and it requires the in situ data. Transient and/or steady state vibration database (real time data or offline data in frames) such as displacements, velocities and/or accelerations is a useful resource for this purpose. Yet growth assessment remains to be a challenging problem. Growth retardation is possible when the tensile and compressive action at the damaged spring is minimized. Hence the problem is posed as follows. When unknown damage is present in one of the linear springs of a discrete structure, in this paper, in situ localization is pursued and then its growth is mitigated by applying the linear quadratic regulator (LQR) design. Although the technique applies to multiple damages with an unknown structural load, in this paper only single damage and transient vibrations are considered. Another important requirement for damage growth retardation is to keep the real parts of the eigenvalue distributions of the damaged structure farther at the left half plane of the complex plane compared to the pristine structure. This requirement depicts robust alpha stability problem. A discrete structure is considered for illustrating several of these features considered in this paper.

Key words: In situ damage detection, growth retardation, vibration data, robust alpha stability.

[1] NRC Research Associate, Dept. of Electrical and Computer Engineering, E-mail: chimpalthradi@gmail.com
[2] Associate Professor, Dept. of Electrical and Computer Engineering, E-mail: george.york@usafa.edu

1. Introduction

A wide range of structural health monitoring (SHM) problems focuses on damage detection [1-3], localization [4-7], assessment [8,9], and mitigation [10,11] under various loading conditions. A structure with damage is often detected during service intervals in offline although the damage occurs in real-time. Thus from the time the damage is occurred to the time the damage is detected, a structural failure with damage growth can happen. In this context, in situ damage localization and damage growth retardation becomes an important problem. It helps to extend the remaining service life of the structure. For damage growth retardation, note that model prediction by damage assessment is required to determine an actuator load and mitigate damage growth online at least until a repairing or a replacement is performed. Hence, damage localization and damage growth retardation continue to be one of the important SHM problems. Consider a discrete dynamic structure made of several springs, masses, and damper components operating with a vibration (transient or steady-state) database. These systems, for instance, may represent the flexible multi body belt drive system modeled using a technique such as the Lagrangian approach [12]. In large scale systems, the structure may consist of several springs and if one of the springs is damaged, then the whole system may lead to a failure. It is also important to check periodically the health of each spring. In these scenarios, assuming that one of the linear springs of the structure is required to be monitored for possible damage, new procedures, based on the fact that the reduced stiffness at the damaged spring exhibit more displacement activity, are captured using hat functions defined for that spring [10]. In this paper, in situ damage localization is pursued by applying this technique and after the damage is localized, damage growth retardation is pursued using the LQR formulations [13]. Vibration

database is utilized for damage localization. In retardation, a fact based on the robust alpha stability criterion to restrict the eigenvalue distributions of the damaged structure, whether controlled or uncontrolled, is applied to limit the damage growth beyond which the structure may vibrate worse than the pristine structure. Here alpha refers to the real part of the eigenvalue of the pristine structure that is nearest to the imaginary axis.

Model updating for damage growth retardation is possible when stiffness loss at the spring is known as an indication of damage. Stiffness loss due to damage is extensively analyzed in composite structures [14-18]. If finite elements are used, stiffness loss introduces perturbations to the finite element stiffness matrix distributions across the continuous structure. In discrete structures, depending upon the damaged spring, the stiffness matrix will exhibit a distribution matrix at which the stiffness of the spring will get deteriorated. The vibration database is utilized to determine the distribution matrix [10]. Hence the model is updated with the damage size. The hat functions considered in this paper to determine spring stiffness loss in the stiffness matrix also applies to continuous structures if vibration based SHM techniques pursued in the literature [19-21] suggest various uncertain finite element stiffness loss distributions across the continuous structure. Yet, a disadvantage with the present method in [10], even for discrete structures, is that displacements at all locations of the masses are assumed available. In state feedback format, the technique may be pursued further by estimating all the states variables using an observer. One of the merits of this approach is that the damage localization technique is numerically attractive. However, the pristine stiffness data of the springs are assumed to be known perfectly. In practice, when the structure becomes old, the stiffness of the linear springs could have been deteriorated. In this case, multiple damage localization becomes important. Hence the approach presented in this paper does accommodate these scenarios of the SHM [10]. Although the procedure

presented in this paper is extendible to multiple springs, presently, damage localization and retardation is pursued when one spring at a time is considered to be damaged.

After the damaged spring is identified, the second objective of this paper is to retard the damage growth so that the amount of stiffness loss in the damaged spring is minimized during its operation. The hat functions derived previously for in situ damage detection are further utilized to minimize the tension and compression activity (can be defined as transient fatigue cycles similar to the structural responses resulting from a fatigue load). Although LQR is suitable to handle hat functions associated with the tensile and compressive forces (contributing to potential energy) and their rates (transient fatigue rate cycles contributing to the kinetic energy) so that the activity at the damaged spring is minimized, the question arises on the linear model to be used to design LQR. As long as the unknown eigenvalues of the closed loop system matrix for the damaged model are farther to the left half plane of the complex plane compared to the pristine model's eigenvalues, it is known that transients of the controlled structure with damage decay at faster rate than the uncontrolled pristine structure. Therefore, it is the real eigenvalue of the damaged structure that must be kept farther from the eigenvalue of the pristine structure which is nearest to the imaginary axis. Again damped frequency (imaginary part of the uncertain eigenvalue hopefully residing in open left half plane of the complex plane) of oscillations contributes to damage growth retardation. Presently only real part restrictions are imposed. This investigation leads to the determination of potential damage sizes that will make the eigenvalues of the damaged structure to cross alpha limit which is the eigenvalue of the pristine structure nearest to the imaginary axis. In this paper, these damage sizes are presented using robust stability analysis [22]. In real time, techniques using EKF are reported in the literature [23-25] to estimate these parameters. When the model is updated with the potential stiffness loss parameters

[26,27], actuator loads to mitigate damage using complete or partial pole placement or adaptive control are presented [28,29]. In this paper, LQR is performed to minimize potential and/or kinetic energy type of functions when hat functions are utilized. Then, using alpha stability criterion, admissible damages for damage growth retardation are presented.

The paper is organized as follows. In Section 2, in situ structural damage localization problem is considered. After the damage is localized, in Section 3, damage growth retardation using LQR design is pursued by using the pristine model. Then admissible damages retarding the damage growth are presented in Section 4. Simulations and conclusions are presented in Sections 5 and 6, respectively.

2. Discrete In Situ Structural Damage Localization

In this section, a problem formulation for in situ damage localization using a vibration database available in real time as a raw data or as a stored database in frames is presented. Consider a second order spring-mass-damper system representing the mechanical systems such as the one considered in [10,11,28] and shown in Figure 1 as follows,

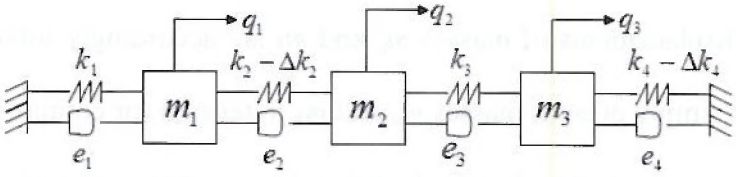

Figure 1 A Discrete Structure Representing a Mechanical System for Damage Localization in Either Spring 2 or Spring 4

$$\mathbf{M}\ddot{\bar{\mathbf{q}}}(t)+\mathbf{C}_0\dot{\bar{\mathbf{q}}}(t)+\mathbf{K}_0\bar{\mathbf{q}}(t)=0,\quad \bar{\mathbf{q}}(0)\neq\mathbf{0} \tag{1}$$

where $\bar{\mathbf{q}}(t)\in R^{\bar{n}}$ is a vector containing $\bar{n}$ damage-free structural degrees of freedom; $\dot{\bar{\mathbf{q}}}(t)$ and $\ddot{\bar{\mathbf{q}}}(t)$ respectively represent the velocity and acceleration of $\bar{\mathbf{q}}(t)$. $\mathbf{M}$, $\mathbf{K}_0$ and $\mathbf{C}_0$ are mass, stiffness and damping matrices that are symmetric with order $\bar{n}$. Consider a linear spring at which one

wants to detect the damage. If a single damage is present at the j^{th} spring, uncertainties Δk_j are introduced in the stiffness and damping matrices as below,

$$\mathbf{K} = \mathbf{K}_0 - \Delta k_j \mathbf{K}_j .$$

$$\mathbf{C} = \mathbf{C}_0 - \Delta e_j \mathbf{C}_j .$$

$\mathbf{K}_j$ and $\mathbf{C}_j$ are the known distribution matrices that can be determined using the stiffness and damping matrices $\mathbf{K}$ and $\mathbf{C}$. The second order system in Eq. (1) is accordingly modified as:

$$\mathbf{M}\ddot{\mathbf{q}}(t) + \mathbf{C}\dot{\mathbf{q}}(t) + \mathbf{K}\mathbf{q}(t) = 0, \quad \mathbf{q}(0) \neq 0 \qquad (2)$$

Note that the states with the damage are denoted by $\mathbf{q}(t)$. Damage detection (or localization) at spring j (to develop the technique assume the damper is healthy) using the vibration database is formulated as follows. Assume $\mathbf{q}(t)$ are measurable or estimated using an observer. Due to the stiffness loss at spring j, it is expected that the displacements of the masses between the spring j are more for damaged system in Eq. (2) than the pristine system in Eq. (1). This behavior of the damaged spring can be studied best by using the isolated hat functions (IHFs) as depicted in Fig. 2. Let k_j be the spring j between masses m_a and m_b. Consistent with the Figure 1, the positive directions of the displacements of masses m_a and m_b are accordingly inferred by $q_a(t)$ and $q_b(t)$, respectively. IHFs simply present masses m_a and m_b in tension (or compression). For instance the IHF in Fig. 2a represents the damaged spring in compression with positive displacement direction for $q_a(t)$ and negative for $q_b(t)$. In the following sections, a procedure based on these IHFs to localize damage is presented.

In order to investigate displacements during compressive and tensile loads at spring j, define the modal vector for masses m_a and m_b as $[\mathbf{x}_m] = \frac{1}{\ell_v}[0 \ \cdots \ -\ell \ \ m \ \cdots \ 0]'$ (prime indicates transpose of the vector). Here, ℓ_v represents the length of the vector $[\mathbf{x}_m]$. ℓ and m are the displacement

units for the masses m_a and m_b, respectively. The orthonormal vector will be $[\mathbf{x}_n] = \frac{1}{\ell_v}[0 \quad \cdots \quad m \quad \ell \quad \cdots \quad 0]^T$. This modal vector depicts the masses m_a and m_b in phase. Note that the modal vector $[\mathbf{x}_m]$ depicts the tensile load using the hat function at Figure 2b. The compressive load is inferred as follows. Define an isolated modal matrix $\mathbf{T}$ as,

$$\mathbf{T} = \frac{1}{\ell_v}\begin{bmatrix} -\ell & m \\ m & \ell \end{bmatrix} \text{ where } \ell, m > 0 \text{ and } \ell_v = \sqrt{\ell^2 + m^2}\,.$$

The displacements $q_a(t)$ and $q_b(t)$ are related by the isolated modal matrix $\mathbf{T}$ as below,

$$\begin{bmatrix} q_a(t) \\ q_b(t) \end{bmatrix} = \mathbf{T}\begin{bmatrix} c_a \\ c_b \end{bmatrix}. \tag{3}$$

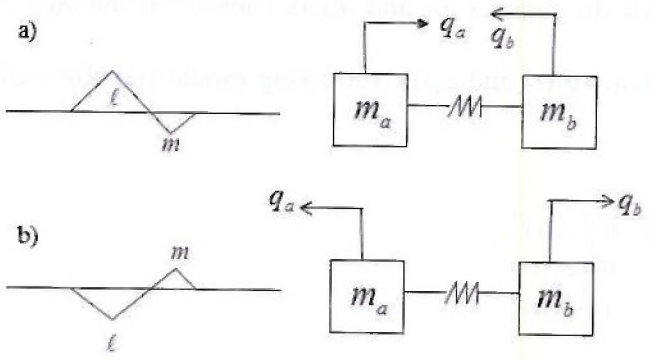

Figure 2 IHFs for a) compressive and b) tensile load tests in spring j

Clearly, when c_a is negative, the spring j takes compressive load. Damage detection criterion at the spring j using the vibration database $q_a(t)$ and $q_b(t)$, IHFs and isolated modal matrix $\mathbf{T}$ is presented. Initial condition response is employed to establish a damage detection criterion. When the vibration database $\mathbf{q}(t)$ due to an initial condition is given, the displacements $q_a(t)$ and $q_b(t)$ connected to the spring j through masses m_a and m_b, respectively, are known to be measured or estimated using an observer. Through the isolated modal matrix $\mathbf{T}$, the constraint in Eq. (3) is established. Note that the vectors,

$$\mathbf{v} = \frac{1}{\ell_v}[-\ell \quad m] \text{ and } \mathbf{w} = \frac{1}{\ell_v}[m \quad \ell], \tag{4}$$

are orthonormal as in the case of modal vectors for an undamped, uncontrolled free vibration problem. For example, consider the case $\bar{n} = 3$. As in the case of a modal matrix, the vectors **v** and **w** form an orthonormal basis for R^3 as given below:

$$\begin{bmatrix} q_1(t) \\ q_2(t) \\ q_3(t) \end{bmatrix} = \begin{bmatrix} 0 & 0 & 1 \\ -\ell/\ell_v & m/\ell_v & 0 \\ m/\ell_v & \ell/\ell_v & 0 \end{bmatrix} \begin{bmatrix} c_1(t) \\ c_2(t) \\ c_3(t) \end{bmatrix} \tag{5}$$

For $\ell > m$, tension and compression with displacement $q_2(t)$ are considered for analysis. For $m > \ell$, tension and compression with displacement $q_3(t)$ are considered for analysis. In this case, a linear spring between the masses m_2 and m_3 is chosen for damage detection. Similarly, for a spring with displacements $q_1(t)$ and $q_2(t)$, following modal transformation can be considered for damage detection.

$$\begin{bmatrix} q_1(t) \\ q_2(t) \\ q_3(t) \end{bmatrix} = \begin{bmatrix} -\ell/\ell_v & m/\ell_v & 0 \\ m/\ell_v & \ell/\ell_v & 0 \\ 0 & 0 & 1 \end{bmatrix} \begin{bmatrix} c_1(t) \\ c_2(t) \\ c_3(t) \end{bmatrix} \tag{6}$$

These transformation matrices can be inferred for a generic displacement vector $\mathbf{q}(t)$ with $\bar{n}$ components. In order to detect damage in the spring j, vibration database for pristine and damaged structures are assumed given. This is a valid assumption because prior to damage, pristine vibration data is available anyway. The following activity indices for the spring j with displacement $q_a(t)$ are defined.

$$\bar{\alpha}_c = \sum |\bar{c}_a(t)|, \quad \text{where } \bar{c}_a(t) < 0 \text{ and } \ell > m \tag{7a}$$

$$\bar{\alpha}_t = \sum |\bar{c}_a(t)|, \quad \text{where } \bar{c}_a(t) > 0 \text{ and } \ell > m \tag{7b}$$

The subscripts 'c' and 't' refer to the compression and tension activity in the spring j. The absolute value of the quantity $\bar{c}_a(t)$ is denoted by $|\bar{c}_a(t)|$. The bar over the coefficients $c_a(t)$ is an indication of the pristine vibration database relation,

$$\begin{bmatrix} \bar{q}_a(t) \\ \bar{q}_b(t) \end{bmatrix} = \mathbf{T} \begin{bmatrix} \bar{c}_a(t) \\ \bar{c}_b(t) \end{bmatrix} \tag{8}$$

Similarly, these activity indices for the spring j with displacement $q_b(t)$ can be inferred by,

$$\bar{\beta}_c = \sum |\bar{c}_a(t)|, \quad \text{where} \quad \bar{c}_a(t) < 0 \text{ and } m > \ell \tag{9a}$$

$$\bar{\beta}_t = \sum |\bar{c}_a(t)|, \quad \text{where} \quad \bar{c}_a(t) > 0 \text{ and } m > \ell \tag{9b}$$

Given the vibration database $\mathbf{q}(t)$ for the damaged structure, the coefficient $c_a(t)$ is computed following the transformation in Eq. (3). Hence the activity indices without bar for the damaged structure are computed as follows.

$$\alpha_c = \sum |c_a(t)|, \quad \text{where} \quad c_a(t) < 0 \text{ and } \ell > m \tag{10a}$$

$$\alpha_t = \sum |c_a(t)|, \quad \text{where} \quad c_a(t) > 0 \text{ and } \ell > m \tag{10b}$$

$$\beta_c = \sum |c_a(t)|, \quad \text{where} \quad c_a(t) < 0 \text{ and } m > \ell \tag{10c}$$

$$\beta_t = \sum |c_a(t)|, \quad \text{where} \quad c_a(t) > 0 \text{ and } m > \ell \tag{10d}$$

The net tensile and compressive displacement activity index (AI) at spring j is defined as,

$$\text{AI} = \sum_i \left|\bar{\alpha}_c^i - \alpha_c^i\right| + \sum_i \left|\bar{\alpha}_t^i - \alpha_t^i\right| + \sum_i \left|\bar{\beta}_c^i - \beta_c^i\right| + \sum_i \left|\bar{\beta}_t^i - \beta_t^i\right| \tag{11}$$

The superscript 'i' is an indication of the vibration database due to various initial conditions. Note that for pristine structures, $\bar{\alpha}_c = \alpha_c$, $\bar{\alpha}_t = \alpha_t$, $\bar{\beta}_c = \beta_c$ and $\bar{\beta}_t = \beta_t$. Thus AI = 0. When the damage is present, however, $\text{AI} \neq 0$. This feature holds even at springs where damage is not present. At the damaged spring, however, AI will be maximal. This property of AI is used to localize the damage in the springs. For the springs connecting the fixed ends, AI is computed in

similar fashion. For instance, consider the first spring in Figure 1. This spring takes compression when $q_1(t)$ is negative and tension when $q_1(t)$ is positive. Thus define,

$$\gamma_c = \sum |q_1(t)|, \quad \text{where} \quad q_1(t) < 0 \tag{12a}$$

$$\bar{\gamma}_c = \sum |\bar{q}_1(t)|, \quad \text{where} \quad \bar{q}_1(t) < 0 \tag{12b}$$

$$\gamma_t = \sum |q_1(t)|, \quad \text{where} \quad q_1(t) > 0 \tag{12c}$$

$$\bar{\gamma}_t = \sum |\bar{q}_1(t)|, \quad \text{where} \quad \bar{q}_1(t) > 0 \tag{12d}$$

The AI for spring 1 will be,

$$\text{AI} = \sum_i \left| \bar{\gamma}_c^i - \gamma_c^i \right| + \sum_i \left| \bar{\gamma}_t^i - \gamma_t^i \right| \tag{13}$$

Note that spring 4 takes compressive load when $q_3(t)$ is positive and tensile load when $q_3(t)$ is negative. Accordingly, the AI in Eq. (13) is computed using the following steps.

$$\gamma_c = \sum |q_3(t)|, \quad \text{where} \quad q_3(t) > 0 \tag{14a}$$

$$\bar{\gamma}_c = \sum |\bar{q}_3(t)|, \quad \text{where} \quad \bar{q}_3(t) > 0 \tag{14b}$$

$$\gamma_t = \sum |q_3(t)|, \quad \text{where} \quad q_3(t) < 0 \tag{14c}$$

$$\bar{\gamma}_t = \sum |\bar{q}_3(t)|, \quad \text{where} \quad \bar{q}_3(t) < 0 \tag{14d}$$

In the next section, the identified damaged spring is considered for growth retardation. Depending upon the spring assumed for damage growth retardation, a mathematical model suitable for LQR design is presented. Note that LQR needs all state variables (displacements and velocities) as measurements. An alternative approach would be to use observers [30,31] where these state variables are estimated depending upon the sensor outputs.

3. Damage growth retardation using LQR

Consider the transformation given in Eq. (5) and (6) for a generic pristine structure as,

$$\bar{\mathbf{q}}(t) = \mathbf{H}\,\bar{\mathbf{c}}(t) \tag{15}$$

such that

$$\dot{\bar{\mathbf{q}}}(t) = \mathbf{H}\,\dot{\bar{\mathbf{c}}}(t) \text{ and } \ddot{\bar{\mathbf{q}}}(t) = \mathbf{H}\,\ddot{\bar{\mathbf{c}}}(t) \tag{16}$$

A finite element model suitable for LQR design in first order from is presented in sequel. Recall the model of the pristine structure compatible with the spring and/or damper damages as,

$$\mathbf{M}\ddot{\bar{\mathbf{q}}}(t) + \mathbf{C}\dot{\bar{\mathbf{q}}}(t) + \mathbf{K}_0\bar{\mathbf{q}}(t) = \mathbf{D}\mathbf{u}(t), \quad \bar{\mathbf{q}}(0) \neq \mathbf{0}.$$

At time $t = 0$, let $\bar{\mathbf{q}}(0)$ be the nonzero initial condition. Without loss of generality, nonzero velocity vectors can also be taken as an initial condition. $\mathbf{u}(t)$ is the control input vector with m components to be determined for damage growth retardation. Substituting Eqs. (15) and (16) in the pristine model,

$$\mathbf{M}\mathbf{H}\ddot{\bar{\mathbf{c}}}(t) + \mathbf{C}_0\mathbf{H}\dot{\bar{c}}(t) + \mathbf{K}_0\mathbf{H}\bar{\mathbf{c}}(t) = \mathbf{D}\mathbf{u}(t) \tag{17}$$

Eq. (17) in first order from is given by,

$$\begin{bmatrix} \dot{\bar{\mathbf{c}}} \\ \ddot{\bar{\mathbf{c}}} \end{bmatrix} = \begin{bmatrix} \mathbf{0} & \mathbf{I}_{\bar{n}} \\ -(\mathbf{MH})^{-1}\mathbf{K}_0\mathbf{H} & -(\mathbf{MH})^{-1}\mathbf{C}_0\,\mathbf{H} \end{bmatrix} \begin{bmatrix} \bar{\mathbf{c}} \\ \dot{\bar{\mathbf{c}}} \end{bmatrix} + \begin{bmatrix} \mathbf{0} \\ (\mathbf{MH})^{-1}\mathbf{D} \end{bmatrix} \mathbf{u}(t) \tag{18}$$

Eq. (18) is the standard structural model in first order form where the tensile and compressive coordinates are considered for the cost function of the LQR. One of the important concerns in this context is to select the actuator placements. For transient vibration monitoring, any actuator placement would work as long as it is used to place eigenvalues that minimize the damage growth retardation. However, for steady state vibration monitoring, actuator placement becomes an important problem as the actuator load is expected to nullify the effects of structural load on the damaged spring by reducing the amplitudes (effect of closed loop pole locations). In practice, it is observed that the transients vanish early but steady state vibration is equivalent to fatigue loads with constant and variable excitation frequency spectrums. Here, it is expected to have the

eigenvalue distribution of the damaged structure farther from those of the undamaged structure in the open left half plane of the complex plane so that fatigue load in controlled structure generate less vibratory amplitudes than the fatigue load in uncontrolled structure. But what eigenvalue locations minimize these effects are unknown and these locations may vary depending upon the number of actuators. In transient case, LQR becomes a powerful tool to determine such eigenvalue locations.

If the model in Eq. (18) is controllable, then the LQR design procedure is recalled briefly. Let Eq. (18) be of the form,

$$\dot{\mathbf{x}}(t) = \mathbf{A}\mathbf{x}(t) + \mathbf{B}\mathbf{u}(t) \tag{19}$$

The control forces at m locations that minimize the cost function $\mathbf{J}$ are given by,

$$\mathbf{u}(t) = -\mathbf{R}^{-1}\mathbf{B}'\mathbf{P}\,\mathbf{x}(t) = -\mathbf{G}\,\mathbf{x}(t) \tag{20}$$

where $\mathbf{P}$ is a positive definite matrix and is the solution of the algebraic Riccati equation,

$$\mathbf{A}'\mathbf{P} + \mathbf{P}\mathbf{A} - \mathbf{P}\mathbf{B}\mathbf{R}^{-1}\mathbf{B}'\mathbf{P} + \mathbf{Q} = \mathbf{0}\,. \tag{21}$$

The positive semi-definite matrix $\mathbf{Q}$ and the positive definite matrix $\mathbf{R}$ are user defined. They define the cost function $\mathbf{J}$ to be minimized as below,

$$\mathbf{J} = \int_0^\infty (\mathbf{x}'(t)\mathbf{Q}\mathbf{x}(t) + \mathbf{u}'(t)\mathbf{R}\mathbf{u}(t))\,dt \tag{22}$$

For the discrete structure shown in Figure 1, the positive semi-definite matrix $\mathbf{Q}$ that minimizes tensile and compressive activity at the damaged spring 2 is selected as follows.

Case A:

$$\mathbf{Q} = \begin{bmatrix} 1 & 0 & 0 & 0 & 0 & 0 \\ 0 & 0 & 0 & 0 & 0 & 0 \\ 0 & 0 & 0 & 0 & 0 & 0 \\ 0 & 0 & 0 & 0 & 0 & 0 \\ 0 & 0 & 0 & 0 & 0 & 0 \\ 0 & 0 & 0 & 0 & 0 & 0 \end{bmatrix} \text{ if } c_1^2(t) \text{ is to be minimized.} \tag{23a}$$

Case B:

$$\mathbf{Q}=\begin{bmatrix}1&0&0&0&0&0\\0&0&0&0&0&0\\0&0&0&0&0&0\\0&0&0&1&0&0\\0&0&0&0&0&0\\0&0&0&0&0&0\end{bmatrix} \text{ if } \bar{c}_1^2(t)+\dot{\bar{c}}_1^2(2) \text{ is to be minimized.} \qquad (23b)$$

For simulations, $\mathbf{R}$ is taken as,

$$\mathbf{R}=0.01\begin{bmatrix}1&0\\0&1\end{bmatrix}.$$

In case A, only spring 2 is assumed to be damaged. Whereas, in Case B, both spring 2 and damper 2 between the masses m_1 and m_2 are assumed to be damaged. Further Case A takes into account only the potential energy. Whereas, Case B, takes into account both potential and kinetic energies. This way the LQR assists to retard the damage growth. However, it is important to observe that the LQR design is pursued using pristine structure and it is applied to the damaged structure. Although the cost function is theoretically not minimized, it is expected that the cost function for the controlled damaged structure is lesser than the cost function for the uncontrolled pristine structure if the eigenvalue distribution of the controlled damaged structure is farther from those of the controlled pristine structure in the left half plane. That is, the eigenvalues of the controlled damaged structure are farther from the eigenvalue of the controlled pristine structure which is nearest to the imaginary axis. This is equivalent to the robust alpha-stability problem under real parameter variations which depict the life of the controlled or uncontrolled structures. In the next section, admissible stiffness and damping parameter variations that would retard damage growth with active control forces determined using LQR are presented.

4. Admissible damages retarding the growth

Consider the damages Δk_2 and Δe_2 introduced in the stiffness and damping matrices as below,

$\mathbf{K} = \mathbf{K}_0 - \Delta k_2 \mathbf{K}_2$ and

$$\mathbf{C} = \mathbf{C}_0 - \Delta e_2 \mathbf{C}_2 \qquad (24)$$

$\mathbf{K}_2$ and $\mathbf{C}_2$ are the known constant distribution matrices. A fundamental problem in damage assessment for structural prognosis is to know the magnitudes of the scalars Δk_2 and Δe_2 for which the eigenvalues with damaged spring and damper are more damped and less oscillatory compared to those eigenvalues with undamaged spring and damper. This theme applies to controlled as well as uncontrolled structures. For the controlled structure, the activity index is expected to be more if the damaged structure with controller exhibits eigenvalues closer to the imaginary axis and away from the real axis compared to the undamaged structure with the same controller. This is the robust alpha-stability problem where alpha is the eigenvalue of the undamaged uncontrolled structure that is closest to the imaginary axis. Note that the farther imaginary parts of the eigenvalues from the real axis contribute to the frequency of oscillations, which also contribute to damage growth and these effects of eigenvalues are currently ignored. The robust alpha stability problem can be posed as follows. Determine the marginal Δk_2 and Δe_2 such that the eigenvalues of the damaged structure with controller exhibit at least one of its eigenvalues on the alpha line parallel to the imaginary axis and the rest of the eigenvalues are alpha stable. Mathematically, these conditions are formulated as follows.

The damaged structure with controller is written as,

$$\dot{\mathbf{x}}(t) = ((\mathbf{A} - \mathbf{BG}) + q_1\mathbf{E}_1 + q_2\mathbf{E}_2)\mathbf{x}(t) = (\mathbf{A}_0 + q_1\mathbf{E}_1 + q_2\mathbf{E}_2)x(t) = \mathbf{A}(q_1, q_2)\mathbf{x}(t) \qquad (25)$$

Here, the matrix $\mathbf{A}_0$ is asymptotically stable with its eigenvalues in the open left half plane of the complex plane. The matrices $\mathbf{E}_1$ and $\mathbf{E}_2$ compatible to $q_1 = \Delta k_2$ and $q_2 = \Delta e_2$ are given by,

$$\mathbf{E}_1 = \begin{bmatrix} \mathbf{0} & \mathbf{0} \\ (\mathbf{MH})^{-1}\mathbf{K}_2\mathbf{H} & \mathbf{0} \end{bmatrix}$$

$$\mathbf{E}_2 = \begin{bmatrix} \mathbf{0} & \mathbf{0} \\ \mathbf{0} & (\mathbf{MH})^{-1}\mathbf{C}_2\mathbf{H} \end{bmatrix} \tag{26}$$

Admissible damages retarding the growth are the admissible $q_i, i = 1,2$ for which the matrix $\mathbf{A}(q_1, q_2)$ is alpha stable (or α – stable). That is, the system with matrix $\mathbf{A}(q_1, q_2)$ is α – stable where α is the real part of the eigenvalue of the matrix $\mathbf{A}$ which is closest to the imaginary axis. Also observe that the fatigue cycles of compressive and tensile activity at the damaged spring are present at matrices $\mathbf{A}(q_1, q_2)$ and at $\mathbf{A}$ in the form the parameters of the hat function in matrix $\mathbf{H}$. In this framework, robust analysis tools discussed in [22] are applied to determine the uncertain parametric values q_i for α – stability. The life of the structure when control is applied will be extended as long as the damage growth with parameters q_i satisfy α – stability. These parametric values assist to monitor the life of the structure which can be estimated using an EKF [10].

5. Simulations

In order to illustrate the underlying principles of structural damage localization and growth retardation in springs, the discrete structure shown in Figure 1 is considered. First damage detection in spring 2 or 3 is performed. In a laboratory setting [32], for a single degree of freedom system, it has been suggested that by measuring amplitudes and frequencies, the displacement is measured. To introduce stiffness loss in the damaged spring, it may be possible to warm up the spring mildly while the displacement measurements are recorded. But for theoretical investigations, the following data is assumed for simulation. $m_1 = 1, m_2 = 2$ and $m_3 = 3$. $k_1 = 10$, $k_2 = 10$, $k_3 = 20$ and $k_4 = 20$. The damping data are $e_1 = 0.5$, $e_2 = 1$, $e_3 = 1$ and $e_4 = 0.5$. For damage detection, a perturbation in spring 2 is introduced. That is, k_2 is changed from 10 to 9 (stiffness loss = 1 unit) , then a vibration database for each initial condition set ($q_1(0)$=0.1, rest are zero; $q_2(0)$=0.1, rest are zero; $q_3(0)$=0.1, rest are zero) were recorded.

Table 1 for spring 2 and Table 2 for spring 3 and Table 3 for springs 1 and 4 summarize the activity indices stated in Eq. (7), Eq. (9), Eq. (10), Eq. (12), Eq. (13) and Eq. (14) respectively. As discussed before, the activity indices α_c, α_t, β_c, β_t, γ_c and γ_t for the damaged structure are different from the pristine structure $\overline{\alpha}_c$, $\overline{\alpha}_t$, $\overline{\beta}_c$, $\overline{\beta}_t$, $\overline{\gamma}_c$ and $\overline{\gamma}_t$. Thus Tables 1, 2 and 3 indicate damage present in the structure. This can be also inferred from the errors $\overline{\alpha}_c^i - \alpha_c^i$, $\overline{\alpha}_t^i - \alpha_t^i$, $\overline{\beta}_c^i - \beta_c^i$, $\overline{\beta}_t^i - \beta_t^i$, $\overline{\gamma}_c^i - \gamma_c^i$ and $\overline{\gamma}_t^i - \gamma_t^i$ in Figures 3 and 4, respectively. The net activity index in Eq. (11) and in Eq. (13) indicates that AI for Table 1 is '2.2653' and for Table 2 is '0.8739'. Similarly, the net activity index in Eq. (13) indicates that AI for Table 3 using springs 1 and 4 is 1.8666 and 0.5326, respectively. The AI against the springs is shown in Figure 5. Since the AI for spring 2 is maximal, it is concluded that spring 2 is damaged.

In the following discussion, damage growth retardation in spring 2 is performed using the LQR. Damage assessment criterion for growth retardation presented in Section 4 is also illustrated in the subsequent discussion. Figure 6 depicts various scenarios by which the transient fatigue cycles can influence damage growth. For instance, the fatigue cycles of an uncontrolled structure (in red) suggest damage growth. Here the stiffness of the spring 2 takes the nominal values. Hence it is categorized as no damage. The transient fatigue cycles of the controlled structure (in blue) suggest damage growth retardation. Once again the simulation is carried out for a nominal spring stiffness value. Hence it is categorized as no damage. Whereas, the transient fatigue cycles of the controlled structure (in black) repeats damage growth retardation scenario; however, an admissible damage size for growth retardation is assumed in the simulations. The admissible damage size is determined based on α – stability criterion discussed in Section 4. The real part of the eigenvalue closest to the imaginary axis when control is not applied is indeed α and it is given by,

$\alpha = -0.08311222\ 3797488$.

Figure 7 depicts the α – stability criterion. The figure considers uncontrolled structure. For the stem values (admissible damage sizes (stiffness and damping loss) for growth retardation), the eigenvalues are preserved with α – stability. That is, for these values, the amplitudes of the transient fatigue cycles with damage in the spring are retained smaller than that of the amplitudes of transient fatigue cycles when there is no damage. In uncontrolled structure, although this phenomenon extends the life of the structure, it is further required that the admissible damage sizes for growth retardation keep the structure non-oscillatory. This requirement depicts the restrictions on the imaginary parts of the eigenvalues, which are difficult to formulate. Also, it is observed that the admissible damping coefficient loss for damage growth retardation increases with stiffness loss. That is when stiffness loss is zero, the admissible damping loss is also zero. When the stiffness loss increases, admissible damping loss also increases reaching the nominal value when $\Delta k_2 = -7$. In the controlled structure, this property is preserved for all stiffness loss with $\Delta k_2 = 0,-1,-2\cdots$, etc. Hence the admissible damage sizes for damage growth retardation are indeed the values at the stems with peak values approaching the nominal values of the spring and damper. Note that for any admissible damage size that might take in real time, the amplitudes of the transient fatigue cycles are always smaller than those of the undamaged structure. This phenomenon also applies to the rate at which transient fatigue cycles change with respect to time as shown in Figure 8.

Next, the above eigenvalue based damage growth retardation discussion is validated with the time responses of $c_1(t)$ and $\dot{c}_1(t)$. In Figure 9, the compression activity is denoted by negative values. These values are sum of $c_1(t)$ over t when $c_1(t) < 0$. Similarly, the tensile activity is denoted by positive values. These values are sum of $c_1(t)$ over t when $c_1(t) > 0$. The uncontrolled

structure exhibit larger values compared to the controlled structure. In both the cases, clearly, damage growth retardation is observed. That is, when stiffness loss increases, the displacement activity also increases. Note that for $\alpha-$stability, the stiffness loss is restricted to 5. In these simulations, the damping loss is assumed zero. Similar observations are recorded with tensile and compressive activity rates in Figure 10. These simulations presented above suggest the validation of the technique for in situ damage localization and damage growth retardation discussed in the paper.

6. Conclusions

Given an operational structure or a mechanical system modeled as a spring-mass-damper system, this paper presents in situ damage localization and assessment with sizes and location of the damage determined completely for damage growth retardation. The new technique for damage localization using isolated hat functions applied to a vibration database is presented. After the damage is localized, damage growth retardation at the spring is pursued using the linear quadratic regulator design. The weighting matrices are particularly attractive to minimize fatigue cycles. But, the design is performed by using a pristine structural model. Hence it becomes necessary to configure damage growth retardation when the model is damaged. This problem is posed as a robust alpha stability problem, where the damage assessment is carried out to guarantee damage growth retardation. A spring mass damper system is considered to illustrate the damage localization and growth retardation problem considered in this paper.

ACKNOWLEDMENT:

This research received no specific grant from any funding agency in the public, commercial, or not-for-profit sectors.

REFERENCES

[1] G. Giridhara, V.T. Rathod, S. Naik, R.D. Mahapatra, and S. Gopalakrishnan, "Rapid Localization of Damage Using a Circular Sensor Array and Lamb Wave Based Triangulation," *Mechanical Systems and Signal Processing*, Vol. 24, No. 8, 2010, pp. 2929-2946.

[2] W.L. Lei, and F.G. Yuan, "Active Damage Localization Technique Based on Energy Propagation of Lamb Waves," *Smart Structures and Systems*, Vol. 3, No. 2, 2007, pp. 201-217.

[3] G. Yan, "A Bayesian Approach for Damage Localization in Plate-Like Structures Using Lamb Waves," *Smart Materials and Structures*, Vol. 22, No. 3, 2013, 035012, doi:10.1088/0964-1726/22/3/035012.

[4] D. Bernal, "Load Vectors for Damage Localization," *ASCE Journal of Engineering Mechanics*, Vol. 128, No. 1, 2002, pp. 7-14.

[5] D. Bernal, "Flexibility-Based Damage Localization from Stochastic Realization Results," *ASCE Journal of Engineering Mechanics*, Vol. 132, No. 6, 2006, pp. 651-658.

.[6] Z. Duan, G. Yan, J. Ou, and B.F. Spencer, "Damage Localization in Ambient Vibration by Constructing Proportional Flexibility Matrix," *Journal of Sound and Vibration*, Vol. 284, 2005, pp. 455-466.

[7] Y. Gao, B.F. Spencer, and D. Bernal, "Experimental Verification of the Flexibility-Based Damage Locating Vector Method," *ASCE Journal of Engineering Mechanics*, Vol. 133, 2007, pp. 1043-1049.

[8] D. Maity, and A. Saha, "Damage Assessment in Structure From Changes in Static Parameter Using Neural Networks," *Sadhana*, Vol. 29, No. 3, 2004, pp. 315–327.

[9] F.N. Catbas, M. Gul, and J.L. Burkett, "Damage Assessment Using Flexibility and Flexibility-Based Curvature for Structural Health Monitoring," *Smart Materials and Structures*, Vol. 17, No. 1, 2008, 015024, doi:10.1088/0964-1726/17/01/015024.

[10] C.R. Ashokkumar, "Active Self-Healing Mechanisms for Discrete Dynamic Structures," *Structural Control and Health Monitoring,* Vol 21, No 5, May 2014, pp. 721-740.

[11] C.R. Ashokkumar, "Vibration Control for Structural Damage Mitigation," *Journal of Vibration and Control*, Published online on January 28, 2014.

[12] G. Cepon, L. Lionel Manin, and M. Boltezar, "Validation of a Flexible Multibody Belt-Drive Model," *Journal of Mechanical Engineering*, Vol. 57, No. 7-8, 2011, pp. 539-546.

[13] B.D. Anderson and J.B. Moore, *Optimal Control: Linear Quadratic Methods*, Prentice Hall, New Jersey, 1990.

[14] M. Kashtalyan, and C. Soutis, "The Effect of Delaminations Induced by Transverse Cracks and Splits on Stiffness Properties of Composite Laminates," *Composites: Part A Applied Science and Manufacturing*, Vol. 31, 2000, pp. 107-119.

[15] E.H. Lim, and T.E. Tay, "Stiffness Loss of Composite Laminates with Transverse Cracks Under Mode I and Mode III Loading," *International Journal of Damage Mechanics*, Vol. 5, No. 2, 1996, pp. 190-215.

[16] L.E. Bogdan, S.H. Yin, E.H. Dowell, "Enhanced Nonlinear Dynamics of Accurate Identification of Stiffness Loss in a Thermo-Schielding Panel," *Nonlinear Dynamics*, Vol. 39, No. 1-2, 2005, pp. 156-162.

[17] T.E. Tay, and E.H. Lim, "Analysis of Stiffness Loss in Cross-Ply Composite Laminates," *Composite Structures*, Vol. 25, No. 1-4, 1993, pp. 419-425.

[18] A. Carpinteri, "Stiffness Loss and Fracture Resistance of a Cracked Beam with Circular Cross Section," *Mechanica*, Vol. 18, No. 3, 1983, pp. 156-162.

[19] D. Montalvao, N.M.M. Maia, and A.M.R. Ribei, "A Review of Vibration-based Structural Health Monitoring with Special Emphasis on Composite Materials," *The Shock and Vibration Digest*, Vol. 38, 2006, 295–324.

[20] C.P. Fritzen, "Vibration-based Structural Health Monitoring – Concepts and Applications," *Key Engineering Materials*, Vol. 293-294, 2005, pp. 3-20. DOI:10.4028/ www.scientific.net/ KEM.293-294.3

[21] S.W. Doebling, C.R. Farrar, M.B. Prime, and D.W. Shevitz, "Damage Identification and Health Monitoring of Structural and Mechanical Systems from Changes in Their Vibration Characteristics: A Literature Review," LA-13070-MS, UC-900, May 1996.

[22] C.R. Ashokkumar, W.P.G. York, and S. Gruber, "A Note on the Counterexamples of Robust Matrix Stability Counterexamples," Submitted, *International Journal of Control*, 8 pages.

[23] J.E. Bauer, and D. Andrisani, *Estimating Short-Period Dynamics Using an Extended Kalman Filter*, NASA-TM-101722, June 1990.

[24] J.L. Speyer, and E.Z. Crues, "Online Aircraft State and Stability Derivative Estimation Using the Modified Gain Extended Kalman Filter," *Journal of Guidance, Control, and Dynamics*, Vol. 10, No. 3, 1987, pp. 262-268.

[25] P. Williams, "Structural Damage Detection from Transient Responses Using Square-Root Unscented Filtering," *Acta Astronautica*, Vol. 63, 2008, pp. 1259-1272.

[26] J.N. Yang, S. Lin, H. Huang, and L. Zhou, "An Adaptive Extended Kalman Filter for Structural Damage Identification I", *Structural Control and Health Monitoring*, Vol. 13, No. 4, 2005, pp. 849-867.

[27] J.N. Yang, S. Pan, and H. Huang, "An Adaptive Extended Kalman Filter for Structural Damage Identifications II: Unknown Inputs," *Structural Control and Health Monitoring*, Vol. 14, No. 3, 2006, pp. 497-521.

[28] C.R. Ashokkumar, and N.G.R. Iyengar, "Partial Eigenvalue Assignment for Structural Damage Mitigation," *Journal of Sound and Vibration*, Vol 330, Issue 1, 2011, pp. 9-16.

[29] C.R. Ashokkumar, B. Dattaguru, and N.G.R. Iyengar, "Adaptive Control for Structural Damage Mitigation," *Global Journal of Researches in Engineering, D Aerospace Engineering*, Vol. 11, No. 5, 2011.

[30] B. Chen, and S. Nagarajaiah, "Observer-Based Structural Damage Detection Using Genetic Algorithm," *Structural Control and Health Monitoring*, Vol. 20, No. 4, 2013, DOI: 10.1002/stc.512.

[31] P. Dharap, B-H. Koh, and S. Nagarajaiah, "Structural Health Monitoring Using ARMarkov Observers," *Journal of Intelligent Material Systems and Structures*, Vol 17, No. 6, 2006, pp. 469-481. DOI: 10.1177/1045389X06058793

[32] D. Boyd, B.D. Schimel, J.L. Ding, M.J. Anderson, and W.J. Grantham, ME 349: Dynamic Systems Laboratory Manuel, School of Mechanical and Materials Engineering, Washington State University, April 1997.

Table 1 Load Test (Pristine/(Damaged)) for Passive Damage Detection in Spring 2

Displacement	$q_1(t)$		$q_2(t)$	
ActivityIndex	$\overline{\alpha}_t/(\alpha_t)$	$\overline{\alpha}_c/(\alpha_c)$	$\overline{\beta}_t/(\beta_t)$	$\overline{\beta}_c/(\beta_c)$
$\sum\lvert c_m(t)\rvert$ $q_1(0)=0.1$	3.9343 (3.9502)	4.6297 (4.6894)	4.0989 (4.0074)	4.5737 (4.5092)
$\sum\lvert c_m(t)\rvert$ $q_2(0)=0.1$	5.7751 (5.3742)	5.2936 (4.8758)	12.2315 (12.4116)	11.7283 (11.8263)
$\sum\lvert c_m(t)\rvert$ $q_3(0)=0.1$	6.8082 (6.4400)	6.6592 (6.3169)	12.6969 (12.8291)	13.1245 (13.2187)

Table 2 Load Test (Pristine/(Damaged)) for Passive Damage Detection in Spring 3

Displacement	$q_2(t)$		$q_3(t)$	
Activity Index	$\overline{\alpha}_t/(\alpha_t)$	$\overline{\alpha}_c/(\alpha_c)$	$\overline{\beta}_t/(\beta_t)$	$\overline{\beta}_c/(\beta_c)$
$\sum\lvert c_m(t)\rvert$ $q_1(0)=0.1$	4.0790 (3.9211)	3.8611 (3.6904)	2.7193 (2.6008)	2.7946 (2.6749)
$\sum\lvert c_m(t)\rvert$ $q_2(0)=0.1$	11.4170 (11.4150)	11.8512 (11.9163)	6.8322 (6.8313)	7.1069 (7.0778)
$\sum\lvert c_m(t)\rvert$ $q_3(0)=0.1$	13.6455 (13.6116)	13.0964 (13.1019)	9.0454 (8.9710)	8.8299 (8.7337)

Table 3 Load Test (Pristine/(Damaged)) for Passive Damage Detection in Springs 1 and 4

Displacement	$q_1(t)$		$q_3(t)$	
Activity Index	$\bar{\gamma}_t/(\gamma_t)$	$\bar{\gamma}_c/(\gamma_c)$	$\bar{\gamma}_t/(\gamma_t)$	$\bar{\gamma}_c/(\gamma_c)$
$\sum \lvert q_i(t) \rvert$ $q_1(0) = 0.1$	6.0424 (6.0320)	5.4054 (5.3537)	4.1319 (3.9857)	3.9564 (3.8066)
$\sum \lvert q_i(t) \rvert$ $q_2(0) = 0.1$	9.8675 (9.4312)	10.2396 (9.7980)	11.6773 (11.6182)	11.5232 (11.5240)
$\sum \lvert q_i(t) \rvert$ $q_3(0) = 0.1$	12.0426 (11.5874)	12.3883 (11.8873)	13.9516 (13.8425)	13.9901 (13.9225)

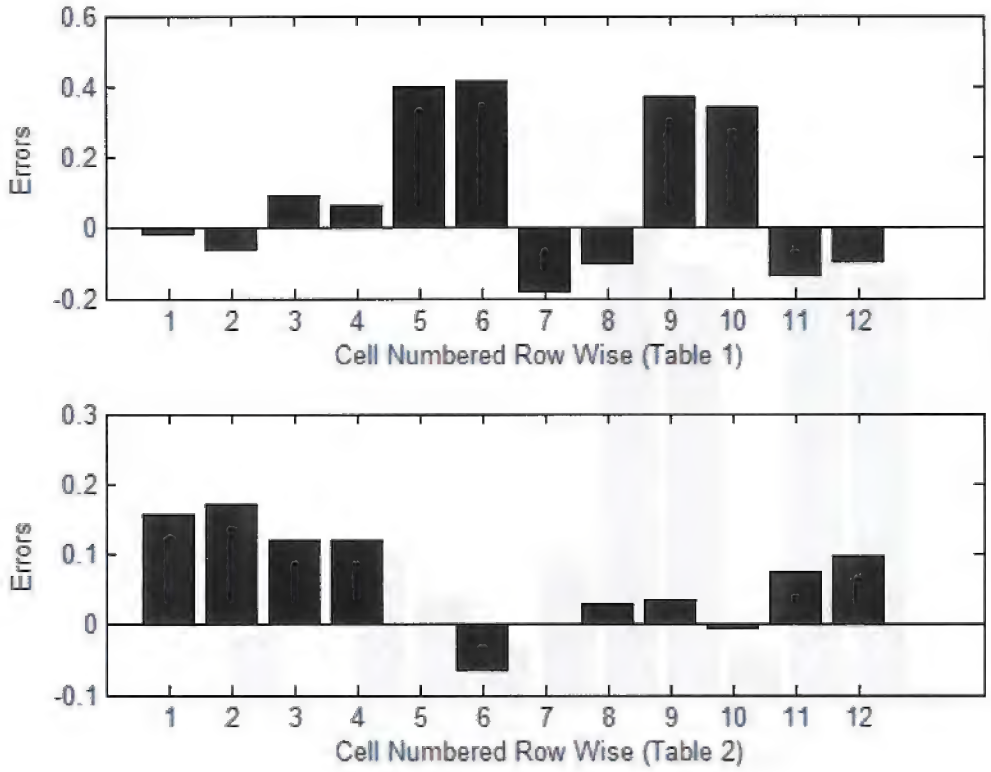

Figure 3 Errors Contributing to Activity Index in Eq. (11)

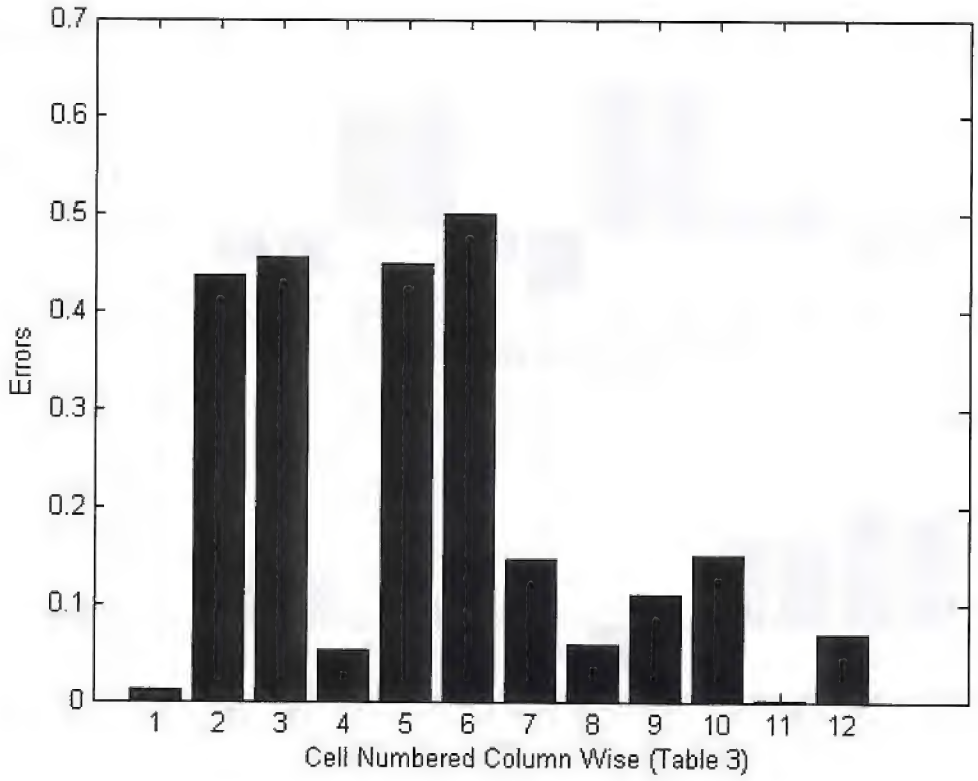

Figure 4 Errors Contributing to Activity Index in Eq. (13).

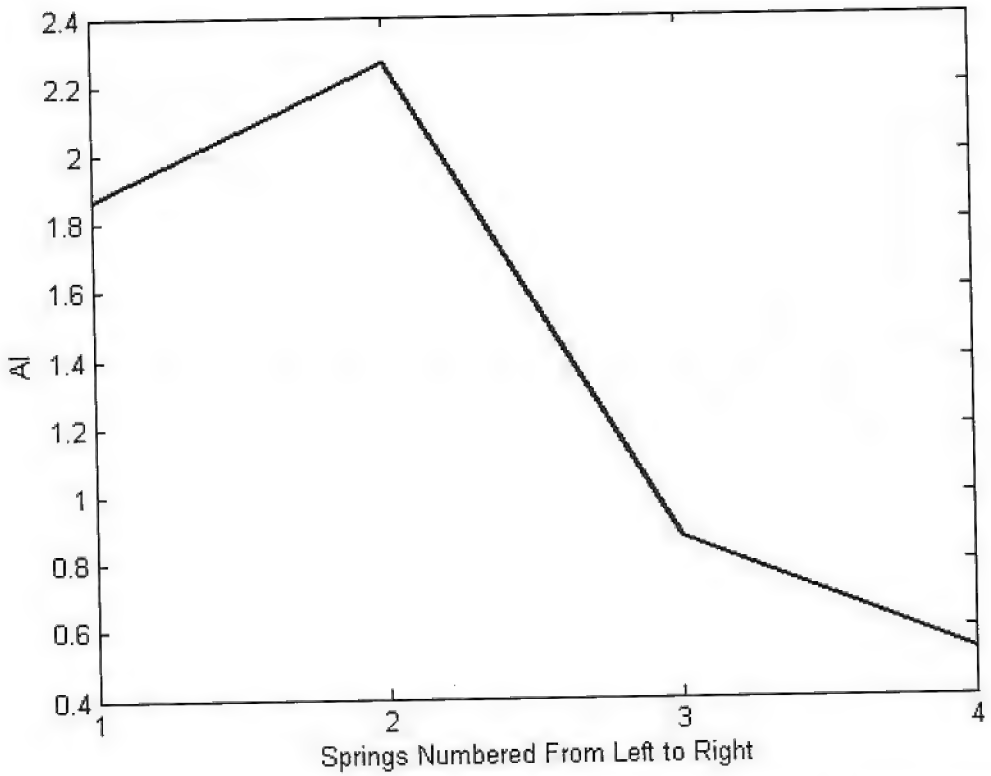

Figure 5 Damage Localization Using Maximal Activity Index (AI) at Spring 2 for a Given Vibration Database From the Structure in Figure 1.

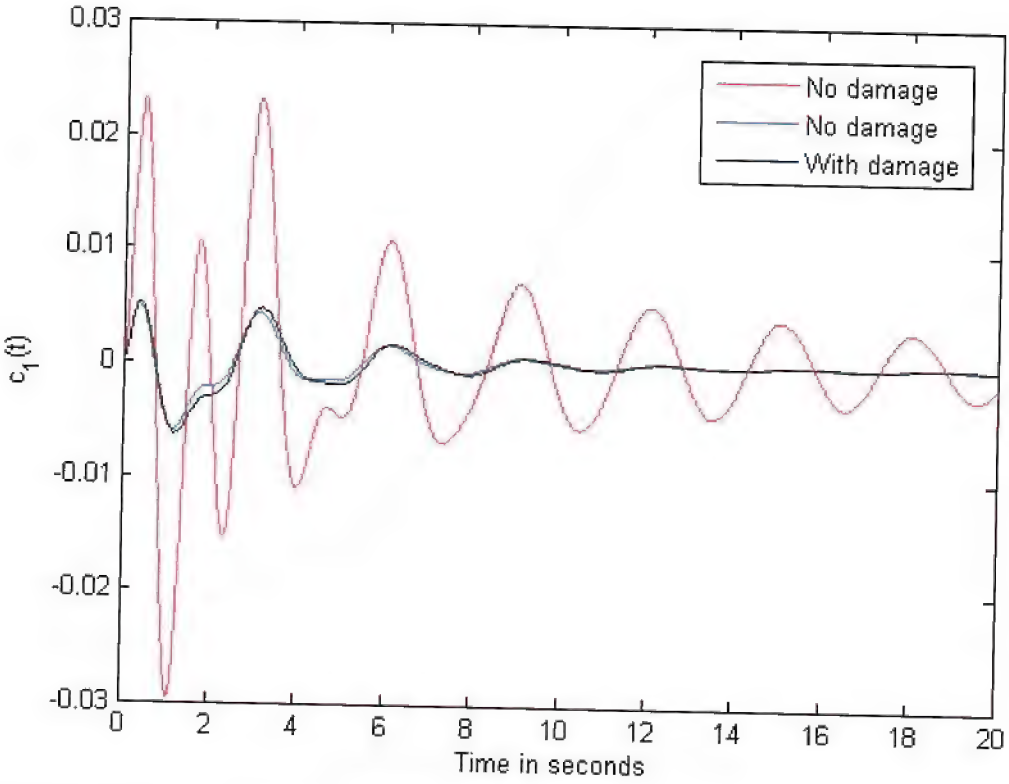

Figure 6. Uncontrolled (red) and controlled (blue and black) fatigue cycles favoring (red) and retarding (blue and black) the damage growth in spring 2.

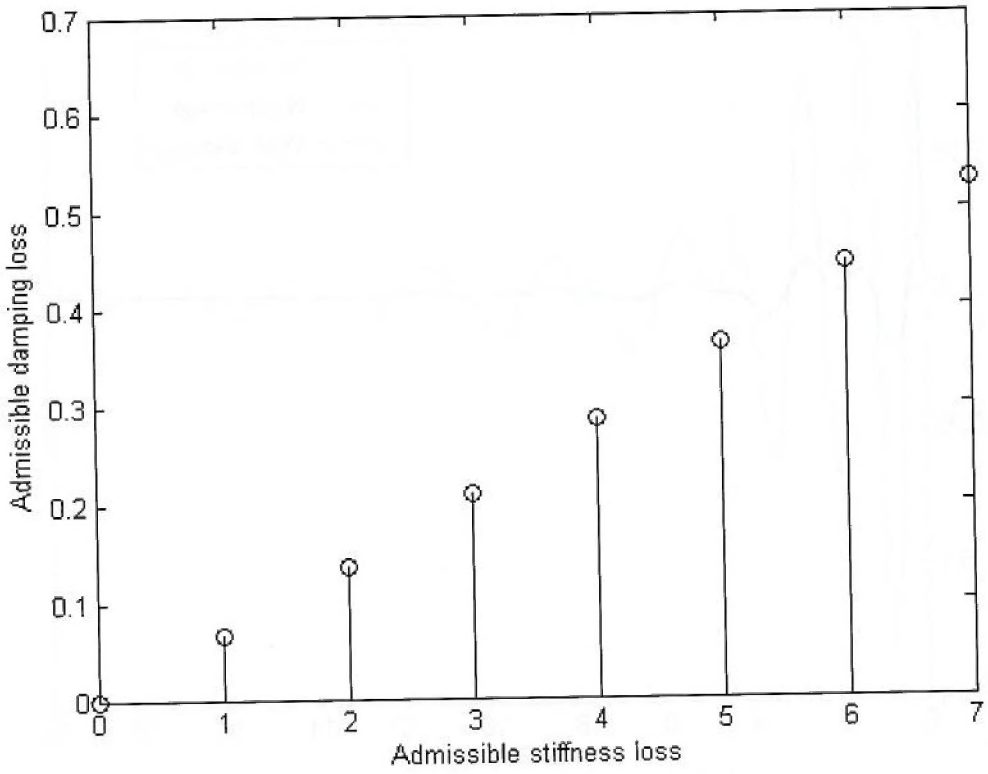

Figure 7. Admissible damages that preserve growth retardation in uncontrolled structure.

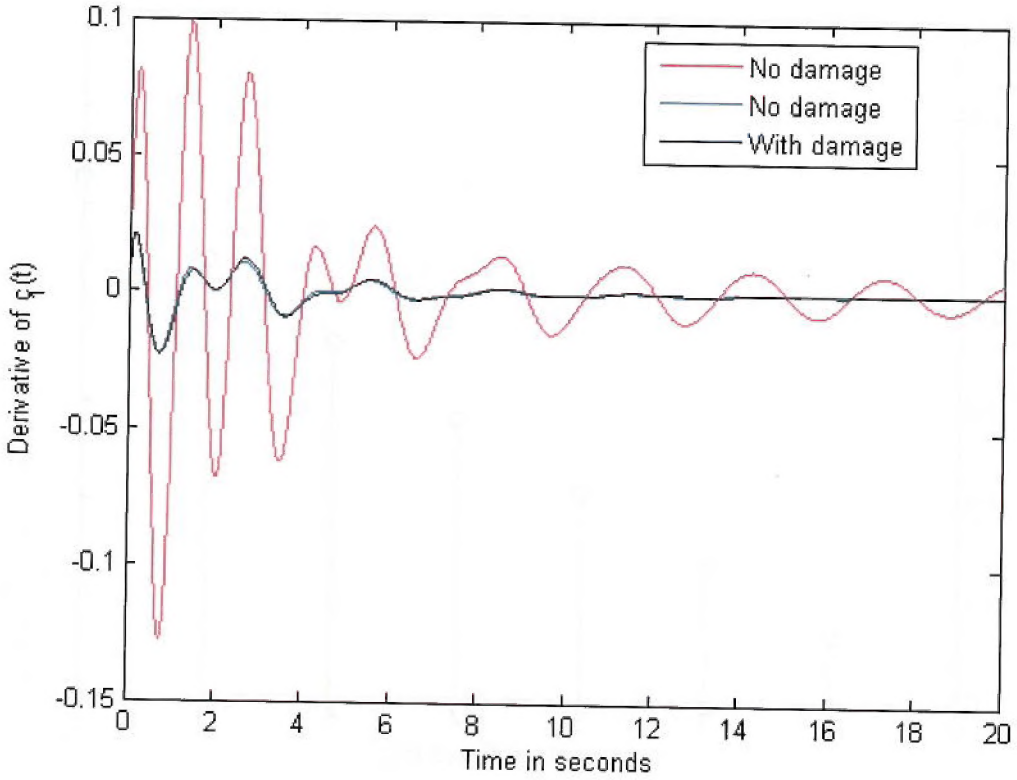

Figure 8. Uncontrolled (red) and controlled (blue and black) fatigue rates favoring (red) and retarding (blue and black) the damage growth in spring 2.

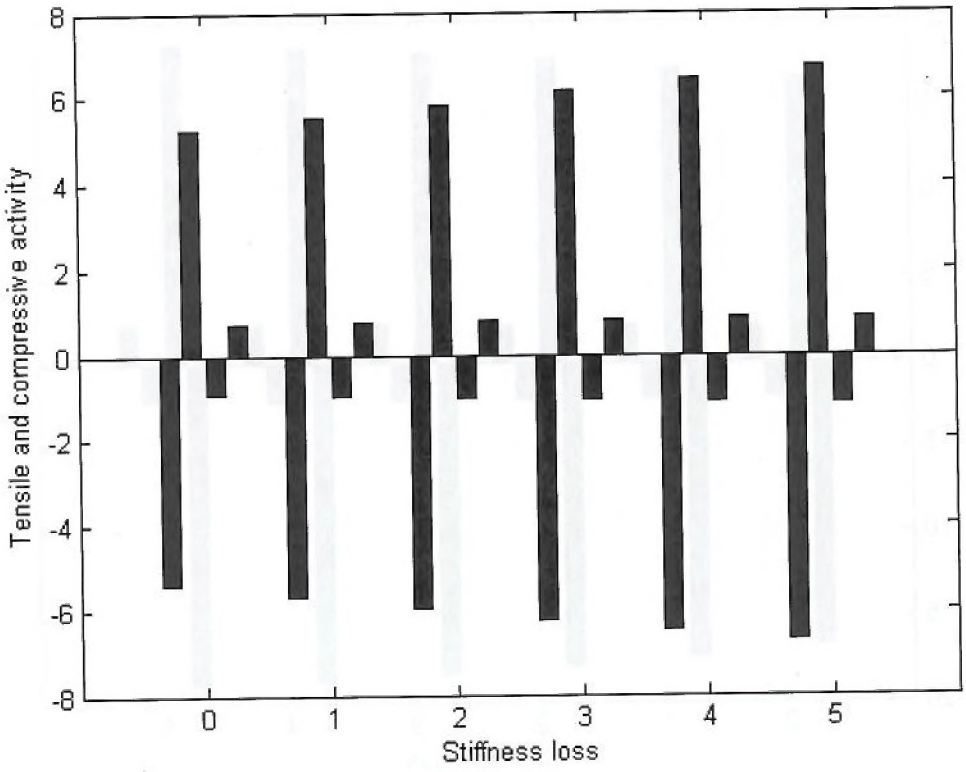

Figure 9: Robust alpha-stability criterion for damage growth retardation validated by displacement activity.

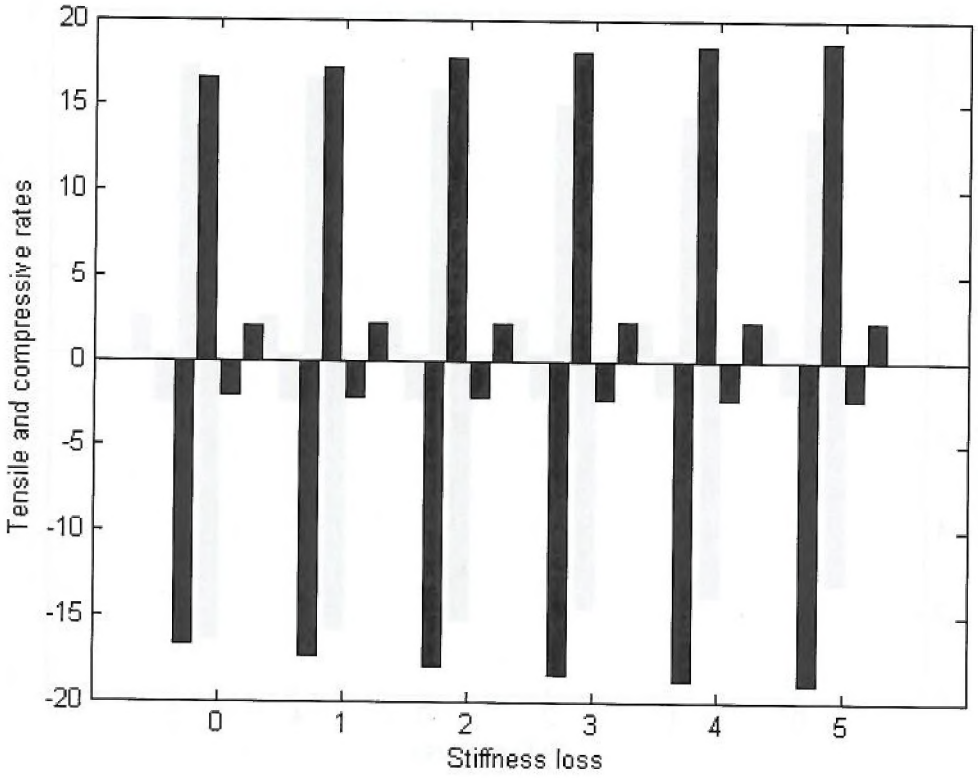

Figure 10: Robust alpha-stability criterion for damage growth retardation validated by velocity activity.